



# Evaluation of Antioxidant Activity and Histopathological Changes Occurred by the Oral Ingestion of CuO Nanoparticles in Monosodium Urate Crystal-Induced Hyperuricemic BALB/c Mice

Mubin Mustafa Kiyani<sup>1</sup> · Maisra Azhar Butt<sup>2</sup> · Hamza Rehman<sup>3</sup> · Moheen Mustafa<sup>4</sup> · Abdul Ghafoor Sajjad<sup>5</sup> · Syed Sajid Hussain Shah<sup>6</sup> · Tariq Mahmood<sup>7</sup> · Syed Ali Imran Bokhari<sup>3</sup>

Received: 11 September 2020 / Accepted: 27 January 2021

© The Author(s), under exclusive licence to Springer Science+Business Media, LLC part of Springer Nature 2021

## Abstract

Nanotechnology is an intensive branch of science due to the unique features of nano range particles (1-100 nm). Their nano size results in a high surface area of absorption when orally administered. Monosodium urate crystal excessive deposition causes a commonly known inflammatory disease called gout into the synovial joints. Previously it has been observed that copper oxide nanoparticles (CuONPs) had a significant effect in reducing the serum uric acid levels in BALB/c mice as well as reducing the inflammation in the ankles of mice. This study was made to investigate the antioxidant and histopathological changes in hyperuricemic BALB/c mice upon the oral administration of copper oxide nanoparticles. Different concentrations of copper oxide nanoparticles 5, 10, and 20 ppm were given orally to gouty mice. To investigate the antioxidant activity of CuONPs, various antioxidant protocols were applied. It was noted that the nanoparticle-treated group of 20 ppm showed no significant changes in superoxide dismutase (SOD), peroxidase (POD), catalase (CAT), thiobarbituric acid reactive substances (TBARS), and ROS values while the protein estimation values of the negative control group exhibited a significant increase (0.001). When compared to negative control, no significant effect was shown on the interpretation of histopathological changes of muscles, kidney, and liver tissues.

**Keywords** Antioxidant · Copper · Hyperuricemia · Histopathology · Nanoparticles

## Introduction

In recent years, nanoparticle (NP) synthesis is considered the most important area of research in the field of nanoscience and technology [1]. NPs are playing essential roles in controlling optical, chemical, physical, and electronic properties of nanomaterials [2]. Generally, a particle size less than 100 nm is said to be in nano range [3, 4]. NPs are classified based on their size, composition, shape, and origin. They have high surface reactivity due to the large percentage of atoms [5]. Because of this unique characteristic, they are unexpectedly reactive with biomolecules [6]. NPs have been extensively used in medical and pharmaceutical products such as toothpastes, sunscreen lotions, shampoos, deodorants, and anti-wrinkle creams [7]. Most of the cosmetics even are formulated by using zinc oxide and titanium dioxide NPs [8]. NPs are also reported as a beneficial agent in the field of biotechnology. They are being used against as anti-cancerous, antifungal, antibacterial, antioxidant, and anti-inflammatory agents. It is reported that NPs are also used for targeted drug delivery due to their bioavailability and bio reactivity [9].

✉ Hamza Rehman  
hamzarehman51@gmail.com

<sup>1</sup> Shifa College of Medical Technology, Shifa Tameer-e-Millat University, Islamabad, Pakistan

<sup>2</sup> Faculty of Rehabilitation and Allied Health Sciences, Riphah International University, Islamabad, Pakistan

<sup>3</sup> Department of Bioinformatics and Biotechnology, Faculty of Basic and Applied Sciences, International Islamic University, Islamabad, Pakistan

<sup>4</sup> Faculty of Engineering, Federal Urdu University, Islamabad, Pakistan

<sup>5</sup> Department of Physical Therapy, Shifa Tameer-e-Millat University, Islamabad, Pakistan

<sup>6</sup> Department of Pathology, Northern Border University, Arar, Saudi Arabia

<sup>7</sup> Department of Nanoscience and Technology, National Center for Physics, Islamabad, Pakistan

In gouty arthritis, monosodium urate (MSU) crystals are considered a key component associated with the rise of serum urate content. Gout is characterized by inflammation due to accumulation of MSU crystals within synovial fibroblast which results in mechanical damage of synovial tissues. During inflammation, tumor necrosis factor- $\alpha$  (TNF- $\alpha$ ) [10], chemokines (IL-8), invading neutrophils, local macrophages, and monocytes are responsible for the secretion of pro-inflammatory mediators like interleukin-1 $\beta$  (IL-1 $\beta$ ) [11]. The MSU crystal initiates mast cell degradation that induces inflammation which results in shearing and tearing of adjacent synovial tissues [10].

In addition to the inflammatory process in gouty arthritis, oxidative stress (OS) is one of the important parameters associated with gout. The oxidative stress condition is triggered by the increased production of reactive oxygen species (ROS) and cytokines as they are pro-inflammatory in nature [12]. The generation of ROS is considered an essential constituent in many physiological procedures such as the bactericidal activity of phagocytes, signal transduction, redox state, and modulation of the cell cycle [13]. OS is the fluctuation between ROS production and antioxidant mechanisms [14]. As a result of its high chemical reactivity, ROS can damage various biomolecules, such as membrane lipid peroxidation, in which the oxidation of fatty acids or lipids results in oxygen free radicals such as peroxide and DNA damage and protein oxidative activity [15]. Another source of ROS production in enzymatic reactions is catalyzed by lipoxygenase, NADPH oxidase, cyclooxygenase, xanthine oxidase, and autoxidation of organic compound. NADPH oxidase from neutrophils and macrophages invades the synovial membrane and serves as another significant source of superoxide radical production [16]. This enzyme binds to the membrane and forms a complex by using a membrane (p22phox and gp91phox) and cytosol (p40phox, p47phox, and p67phox)-located subunits. It has been declared that endothelial cells, fibroblasts, and chondrocytes are all responsible for the expression of NADPH oxidase components and produce oxygen free radicals [17]. The oxygen free radicals are responsible for damaging endothelial cells and the extracellular matrix, resulting in the increased migration of neutrophils to the point of inflammation. Free oxygen radicals are converted into hydroxyl radical (HO $\cdot$ ) as more aggressive ROS when it interacts with free Fe $^{+3}$  or Cu $^{+2}$  ions [18]. Peroxidant products, particularly malonyldialdehyde (MDA), have been identified as a secondary mediator for hyaluronic acid depolymerization, collagen degradation, proteoglycan degeneration, protein oxidation, and inhibition of proliferative mechanism in cartilage tissue [19].

Copper is one of the important biologically essential trace elements. At the cellular level, its function is to inhibit xanthine oxidase (XOD) and xanthine dehydrogenase (XDH), which results in the reduction of purine conversion into uric acid [20]. It has been reported from the previous studies that the reduction or overproduction of XOD/XDH increases the

incidence of gout (hyperuricemia) [20, 21]. Copper is also known for its antagonistic effect in comparison with molybdenum. The active site of XOD and XDH is called as molybdopterin. As copper concentration increases, the activity of these enzymes ceases [21]. Previous studies show that copper is also used as an antibacterial agent [22]. It is required for the antioxidant activity, carbohydrate, and xenobiotic metabolism [23]. The xenobiotic metabolism was observed in liver cells of rat when exposed to copper sulfate. It has been observed that copper increases the expression of the genes such as CYP1A1 and CYP1A2 which are involved in the production of enzymes (cytochrome P450) responsible for the xenobiotic activity. Copper is also well-known for its antifungal [24] and anti-inflammatory activities. At the cellular level, copper is considered an essential micronutrient for its protein trafficking and redox property. A recent study has proved the beneficial effects of copper in neurodegenerative diseases. The cellular prion protein (PrPC), which is mostly known as the neurodegenerative protein, is implicated in various biochemical processes, including neuritogenesis. The role of PrPC neuritogenesis is impaired by N copper terminal amino acids directly [25].

CuO-NP has also been reported as a beneficial agent in reducing inflammation due to lung infection [24]. Hyperuricemic effect of copper complexes and its nanoparticles have also been studied in recent years [26, 27]. From a previous study, it has been declared that during inflammation, the rate of oxidative stress increases. One of the studies reported that CuO-NPs are also responsible for the reduction of oxidative stress. *Streptomyces pseudogriseolus* Acv-11 strain was used to prepare CuO-NPs which was responsible for the better response in terms of scavenging and total antioxidant activity [28]. For this purpose, we have designed a study to illustrate the potential effects of CuO-NPs on antioxidant activity and histopathology of MSU-induced gouty BALB/c mice by intra-articular injection of monosodium urate crystals. We also observed the effect of CuO-NPs in comparison with commercially available drug allopurinol for the treatment of gouty arthritis for the reduction of oxidative stress.

## Methods

### Synthesis of CuO-NPs

CuO-NPs were synthesized by using a previously studied chemical reduction method [29]. First, de-ionized water (120 ml) and 1.2% of starch solution were mixed with to make a solution. A 1.2% starch solution was utilized for the preparation of 0.1 M copper sulfate solution. Ascorbic acid (0.2 M) was prepared by using 50 ml of de-ionized water. Under vigorous and continuous stirring using a magnetic stirrer, in copper sulfate solution, ascorbic acid was added gradually. Later

on, de-ionized water (30 ml) was used to prepare (0.1 M) NaOH solution which served as a reducing agent and was added dropwise into the main solution. The temperature of the stirring solution was kept up to 80 °C. After the addition of NaOH, the color of the solution turned from yellow to ochre which indicates the synthesis of copper nanoparticles. These obtained particles were filtered and washed several times with de-ionized water and ethanol. Finally, these particles were dried at room temperature, and this whole process can better be understood by Fig. 1. These copper nanoparticles were used to make 5, 10, and 20 ppm colloidal solutions in de-ionized water which were then orally administered to mice.

## Characterization

UV-Vis spectroscopy (Macy UV-1800PC) was utilized for the detection of copper oxide nanoparticles, and it is the simplest way to confirm the formation of nanoparticles. A colloidal solution of copper nanoparticles was prepared and quartz cuvette was used to detect the absorbance. The absorbance spectrum of the colloidal sample was obtained in the range of 200–800 nm. Structural composition of CuO-NPs was found out by performing X-ray diffraction (XRD) using AXS D8 Advance. This parameter of characterization was

performed to investigate the crystalline structure of CuO-NPs, while the surface morphological and elemental analysis was determined by scanning electron microscopy (SEM) and energy-dispersive X-ray spectroscopy (EDS) using Tescan Vega 3.

## Animal Model

In this experiment, BALB/c mice (25–30 g) were used as a model organism. Thirty-six mice were obtained from the National Institute of Health (NIH), Islamabad, Pakistan, after which they were arbitrarily separated into 6 groups ( $n = 6$ ). All the laboratory conditions were maintained according to the standardized method before initializing the experiment. Mice were kept in cages under 22–25 °C room temperature with 24/7 dark-light cycle. Mice were given diet according to previously studied standards, which contained 6 mg/kg of copper as an essential trace nutrient. The ingredients of the diet are mentioned in Table 1 [30], and 0.1 mg/l of copper was present in the water. Animal's handling protocols and techniques (Letter No. IIU (BI&BT)/FBAS-IBBC-2017-4) were approved by the ethical committee of IIUI department. The dosage scheme with the time interval can be seen in Table 2.

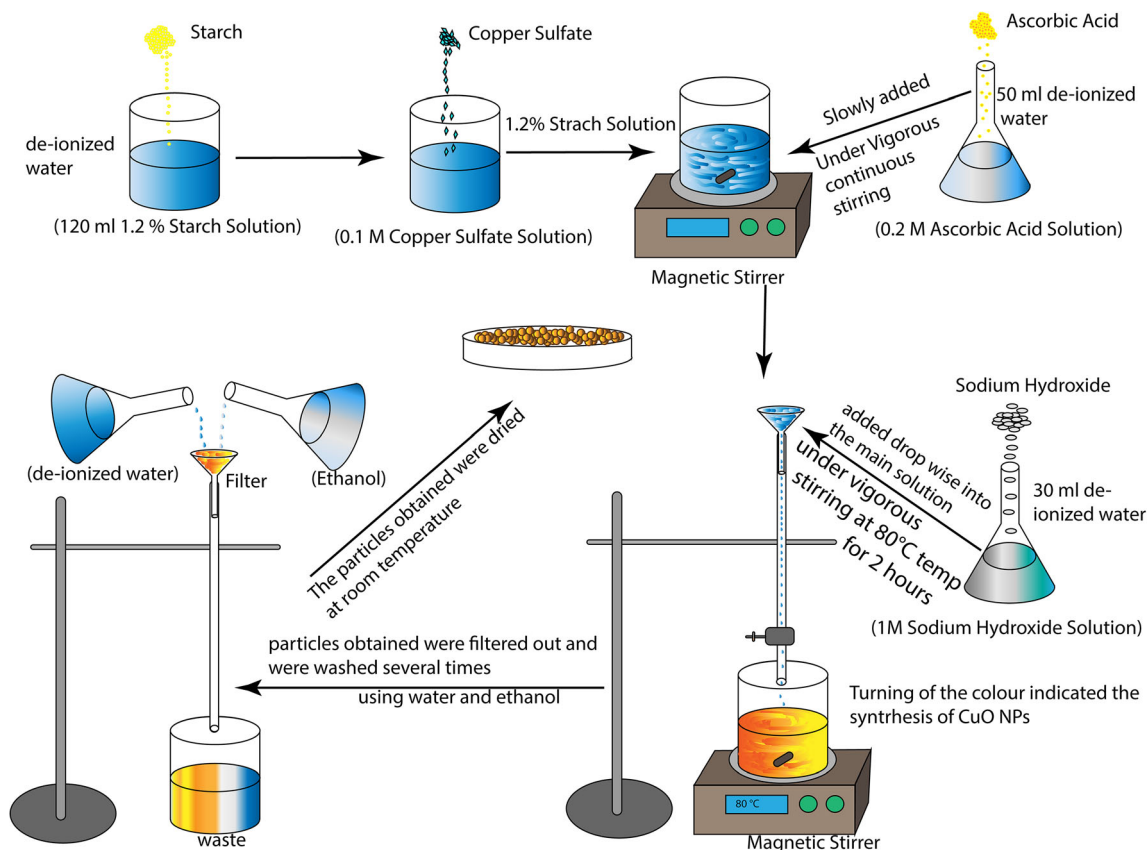


**Fig. 1** Process for the synthesis of copper oxide nanoparticles [29]

**Table 1** The composition of diet given to mice [30]

Ingredients	Growth diet (g/kg diet)	Adult diet (g/kg diet)
Cornstarch	397.486	465.692
Casein (>85% protein)	200	140
Dextrinized cornstarch	132	155
Sucrose	100	100
Soy bean oil	70	40
Fiber	50	50
Mineral mix	35	35
Vitamin mix	10	10
L-Cysteine	3	1.80
Choline bi-tartrate	2.5	2.5
Tert-butylhydroquinone	0.014	0.008

### Synthesis of Monosodium Urate Crystals

MSU crystals were synthesized by using sodium hydroxide (0.001 M) and 1.68 g uric acid. Both of them were mixed at 70 °C temperature. To maintain the pH (7.1-7.2), hydrochloric acid (HCl) and NaOH were added. For the formation of crystals, the whole solution was kept for 24 h at standardized room temperature. The supernatant was discarded and the needle-shaped crystals were washed several times using distilled water [31].

**Table 2** Group details and dosage given to each group

Groups	Time interval	Dose scheme
Control (group 1)	• 8 weeks daily (normal feed)	Normal mice
MSU group (negative control) (group 2)	• Intra-articular injection 3 weeks daily (once) • Intraperitoneal injection 2 weeks (once)	MSU-induced hyperuricemic BALB/c mice
CuO-NP-I (group 3)	• 3 weeks daily (once)	Hyperuricemic orally administered CuONPs 5 ppm
CuO-NP-II (group 4)	• 3 weeks daily (once)	Hyperuricemic orally administered CuONPs 10 ppm
CuO-NP-III (group 5)	• 3 weeks daily (once)	Hyperuricemic orally administered CuONPs 20 ppm
Allopurinol (group 6)	• 3 weeks daily (once)	Hyperuricemic orally administered allopurinol 50 mg/kg body weight

### Allopurinol Dosage

Commercially available allopurinol by the brand name of Zyloric 100 mg was dissolved in de-ionized water. Group 6 hyperuricemic mice were administered with this allopurinol solution at 50 mg/kg body weight dosage with the help of oral gavage. This drug was administered once a day for a period of 3 weeks.

### Experimental Design

In order to find out the antioxidant activity and histopathological changes of CuO-NPs on hyperuricemic BALB/c mice, each group was provided with MSU to induce gouty arthritis, except the control group. For the interval of 3 weeks, MSU was injected inside the ankle joint of the mice. After that, intraperitoneal injections of MSU were provided for the next 2 weeks. This induction of MSU caused inflammation of the ankle joint, resulting in swelling. The diameter of the joints was measured by a vernier caliper. Different concentrations of CuO-NPs were prepared in distilled water by using a sonicator. The 5, 10, and 20 ppm concentrations were synthesized and administered to gouty mice by oral gavage for 3 weeks. A commercially available drug called allopurinol having anti-hyperuricemic effect was administered to the positive control group (50 mg/kg body weight). Previously it was seen that these copper nanoparticles were significant in reducing the serum uric acid levels as well as the swelling of joints in BALB/c mice [27].

### Biochemical Analysis

#### Antioxidant Enzyme Assays

For in vivo study, liver, muscle, and kidney tissues were collected for antioxidant enzyme activity. An automatic homogenizer was used to make a homogenized mixture of tissue in phosphate-buffered saline solution and later on the mixture was centrifuged at 30,000 rpm for about half an hour. After which, the supernatant was separated and utilized for antioxidant enzyme activity and total protein estimation.

#### Catalase

Catalase (CAT) activity was performed by using the method of Chance and Maehly [32] with some modifications. Dilutions were prepared by utilizing a mixture of 2 ml of phosphate buffer at pH = 7.0 and 50 ml of homogenate. The variations in absorbance of the solution were observed at a wavelength of 240 nm. One unit of CAT was defined as a change in the absorbance by 0.01 unit/min.

### Superoxide Dismutase

With some modifications, the method of Kakkar et al. [33] was utilized to calculate superoxide dismutase (SOD) activity. After the reaction occurred in 1 min, readings were noted at 560 nm wavelength from the spectrophotometer. SOD values were presented in U/mg of protein.

### Guaiacol Peroxidase

Peroxidase (POD) activity in the homogenate of tissue was measured after some modifications of the spectrophotometric method of Chance and Maehly [32]. A total of 0.1 ml of homogenate, 0.1 ml of guaiacol, and 2.5 ml and 0.3 ml of H<sub>2</sub>O<sub>2</sub> of phosphate buffer were used in this assay and 470 nm wavelength was used to measure the absorbance. One unit of POD was defined as a change in the absorbance of 0.01 unit/min.

### Lipid Peroxidation by TBARS

Thiobarbituric acid reactive substances (TBARS) activity was calculated in the tissue homogenate and the results were presented in TBARS/min/ml of plasma. Homogenate (0.1 ml), trichloro-barbituric acid (1 ml), trichloroacetic acid (0.1 ml), and phosphate buffer (0.29 ml) were mixed in this assay. This whole solution was heated at 95 °C for 20 min and then again for 10 min. Furthermore, it was shifted to an ice bath before centrifuge (2500 rpm). The spectrophotometer was used to measure absorbance at 535 nm wavelength [34].

### Reactive Oxygen Species

Reactive oxygen species (ROS) assay was performed to identify the tissue damage before and after treatment of hyperuricemia with CuO-NPs. 5 ml each of H<sub>2</sub>O<sub>2</sub>, standards and the homogenate was mixed with 140 ml of sodium acetate buffer solution (pH = 4.8) in a 96-well plate, and this plate was incubated at 37 °C (5 min). N,N'-diethyl-1,4-phenylenediamine (DEPPD) ferrous sulfate (100 ml) and the mixed sample were added according to ratio 1:25 in each well. The plate was incubated again for 1 min at 37 °C. The absorbance was recorded with a break of 15 s for 3 min using a microplate reader at 505 nm wavelength [35].

### Total Protein Estimation

AMEDA laboratory diagnostic kit was utilized for the determination of total protein in the tissue. Liver, muscle, and kidney tissues were obtained for the total protein estimation of protein. The results of total protein were measured by plotting absorbance between the standard values and sample. These protein estimation results were expressed as mg/g of tissue.

### Tissue Histology

Liver, kidney, and muscle tissues were preserved in formalin solution for the time of 48 h. Different concentrations of alcohol and xylene were used to dehydrate the tissue content. The tissues were fixed in paraffin wax and sections (5 mm) were cut. Section cutting of tissues was performed on a microtome. To observe the standard histology and morphometric changes, the sections were stained with hematoxylin and eosin stain. Microscopic evaluation was carried out on 4 samples from each group for muscle, liver, and kidney tissues.

### Statistical Analysis

For the comparison of the data obtained from different groups, Dunnett's multiple comparison test was used which followed analysis of variance (ANOVA), using the IBM SPSS (version 25) software. Values were expressed as mean ± standard deviation and were considered significant at  $P < 0.05$ .

## Results

### Characterization of CuO-NPs

From the XRD analysis, the highest peak was recorded at 36.050° of 2θ at the  $x$ -axis shown in Fig. 2(b) in comparison to the intensity, which shows the existences of copper oxide nanoparticles. Debye-Scherrer equation was utilized to calculate the size of the synthesized nanoparticles which was estimated to be around 45 nm. UV-Vis spectroscopy analysis of copper oxide nanoparticles showed an intense peak around 372 nm as shown in Fig. 2(a). The absorption bands for copper nanoparticles have been reported to be in the range of 550–600 nm [36–38].

SEM of CuO-NPs determined that the synthesized particles were in nano ranges and were also agglomerated. Figure 3 shows that the prepared nanoparticles were round in shape. Measurement of the diameter showed that these particles ranged between 29 and 50 nm.

EDS of CuO-NPs revealed the quantitative analysis of the sample which showed copper was present in adequate amounts. Traces of carbon were also seen. EDS analysis can be observed in Fig. 4.

### Assessment of Antioxidant Profile

#### SOD, POD, and CAT

In the diseased negative control group, the SOD, POD, and CAT values were decreased ( $P < 0.001$ ) significantly in comparison with the normal control as shown in

**Fig. 2** **a** UV-Vis spectrum of synthesized copper oxide nanoparticles. **b** XRD pattern of synthesized copper oxide nanoparticles

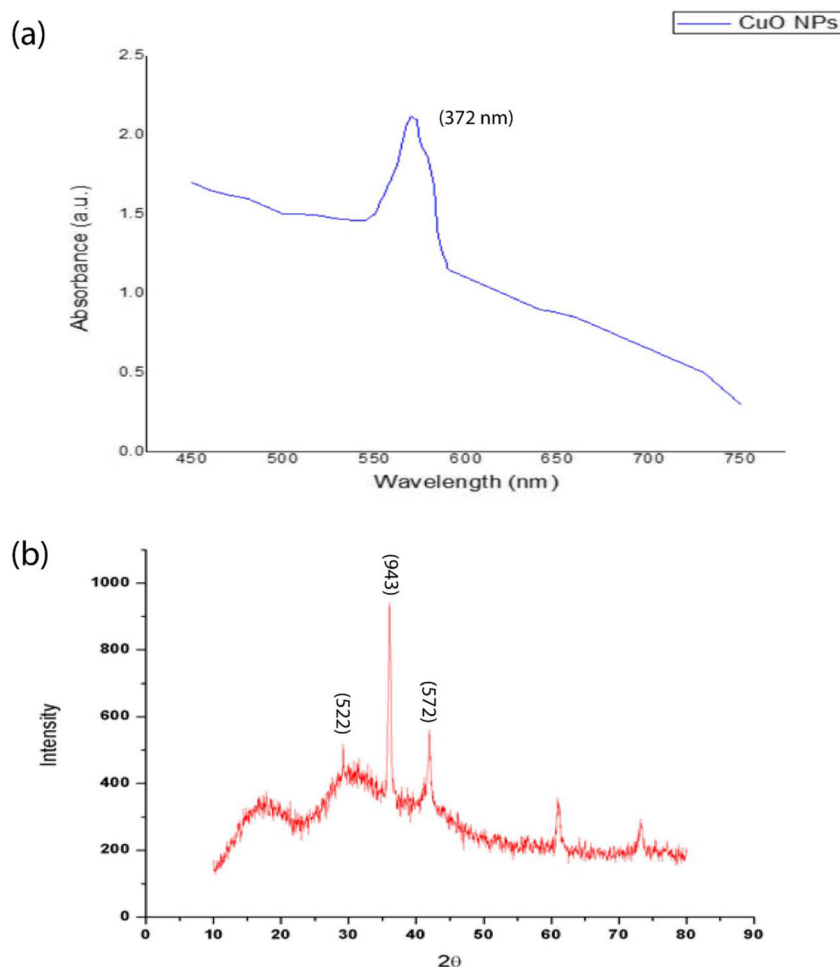


Table 3. The CuO-NP-I-treated group observed a significant decrease ( $P < 0.001$ ) in SOD, POD, and CAT values. Moreover the CuO-NP-II-treated group showed a significant decrease ( $P < 0.001$ ) ( $P < 0.05$ ) in SOD and POD values respectively. The CAT values of the allopurinol-treated group showed a significant decrease ( $P < 0.001$ ) in comparison to the normal control. CuO-NP-III showed a significant increase ( $P < 0.001$ ) when compared with control.

### ROS and TBARS

ROS and TBARS values of the diseased negative control group were highly significant ( $P < 0.001$ ) and increased as compared to the normal control. The CuO-NP-I-treated group observed a significant decrease of  $P < 0.01$  in ROS and  $P < 0.05$  in TBARS values. The CuO-NP-II-treated group showed a significant decrease ( $P < 0.05$ ) in ROS values in comparison with the control. CuO-NP-III showed a significant decrease ( $P < 0.001$ ) when compared with the control (Table 4).

### Total Protein Estimation

The total protein content of the diseased negative group was increased very significantly in comparison with the normal control (Table 5). The other treated groups showed no significant difference in comparison to the controls.

### Histopathology

Mild mononuclear infiltration was observed in kidney tissue of the MSU-induced gouty arthritis group. Some of the interstitial hemorrhages and destruction of epithelial cells in proximal and distal convoluted tubules were also observed. The CuO-NP-treated group (5, 10, 20 ppm) resulted in the reduction of inflammation in kidney tissues. Different doses depicted the reduced loss of epithelial cells. There was significant change observed in liver tissues of the diseased and treated groups. The histopathology of muscle cells of the MSU and nanoparticle-treated groups showed no inflammation and physiological changes in muscle tissues as compared to the control. The changes in histopathology can be seen in Fig. 5.

**Fig. 3** Scanning electron microscope (SEM) image of synthesized copper nanoparticles

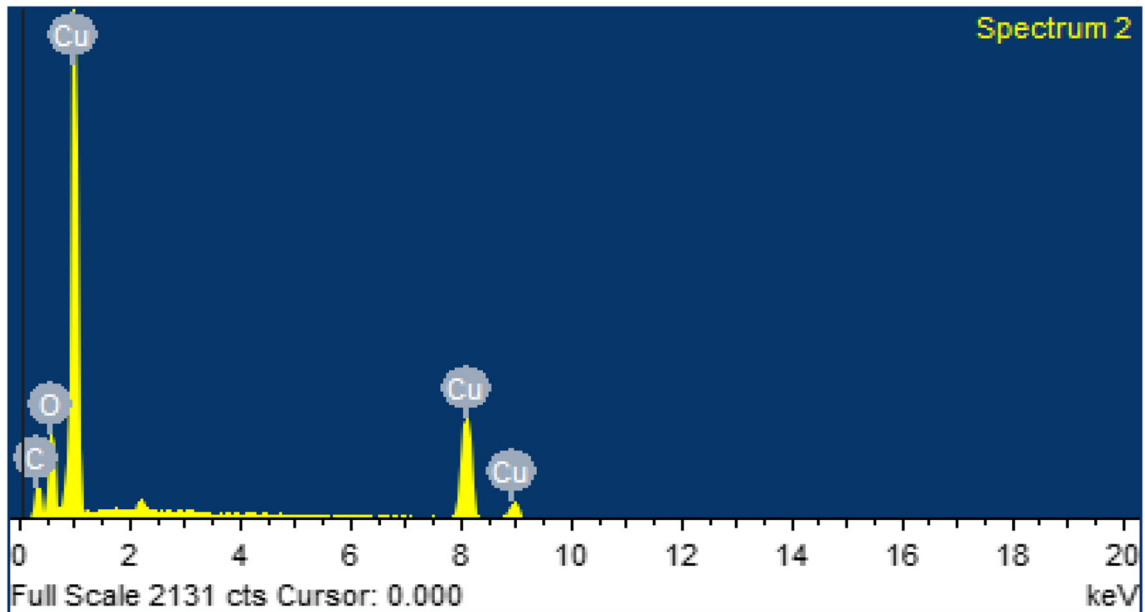
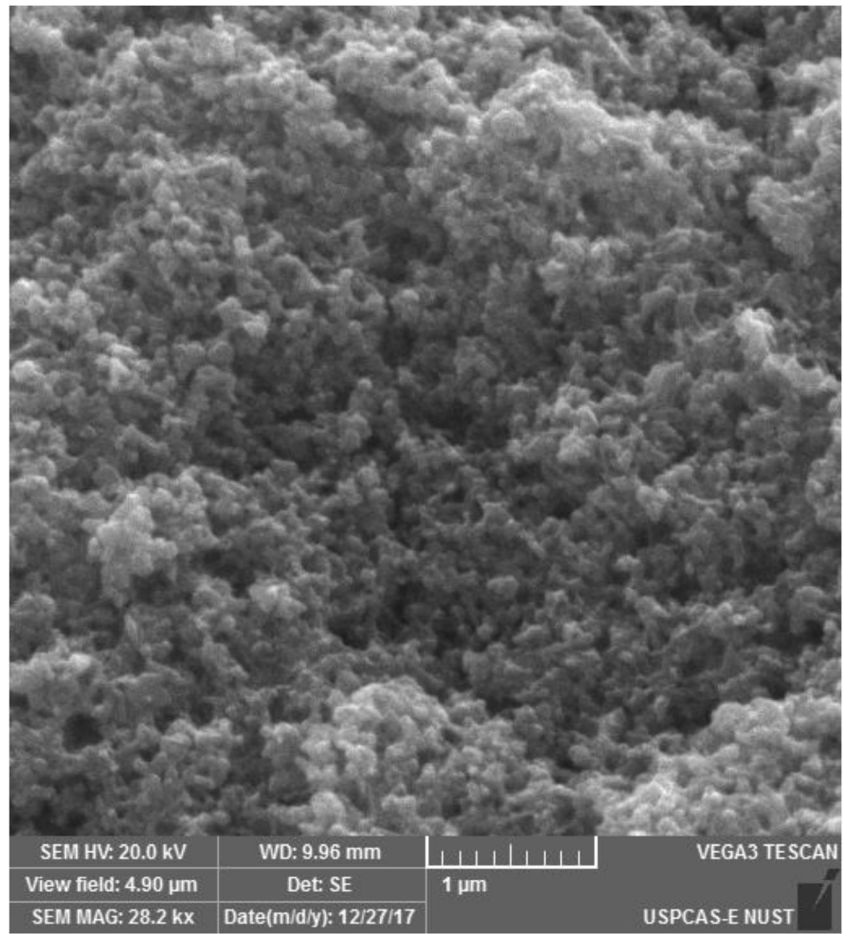


**Fig. 4** Energy-dispersive X-ray spectroscopy pattern of synthesized copper oxide nanoparticle

**Table 3** Results of SOD, POD, and CAT activity of CuONP-administered BALB/c mice

Groups ( <i>n</i> = 6)	Parameters		
	SOD (U/mg protein)	POD (nmol)	CAT (U/mg protein)
Control	34.41 ± 0.8	4.04 ± 0.4	4.33 ± 0.3
MSU group	22.58 ± 0.6***	1.60 ± 0.2***	1.90 ± 0.1 ***
CuO-NP-I	26.01 ± 0.8***	2.45 ± 0.1***	2.57 ± 0.03***
CuO-NP-II	32.65 ± 0.9	3.17 ± 0.1*	3.62 ± 0.1
CuO-NP-III	38.74 ± 0.9***	6.15 ± 0.2***	6.35 ± 0.1***
Allopurinol	32.74 ± 0.7	2.74 ± 0.1	3.01 ± 0.2***

Values are expressed as mean ± SD

\**P* < 0.05

\*\**P* < 0.01

\*\*\**P* < 0.001

## Discussion

CuO-NPs are reported for their antioxidant, antimicrobial, and antifungal characteristics [39]. This study aimed to evaluate the antioxidant activity and histopathology of orally administered CuO-NPs in MSU-induced hyperuricemia. However, there has been no report published regarding the antioxidant activity of CuO-NPs in MSU-induced gouty arthritic mice. Gout was induced by intra-articular administration of monosodium urate (MSU) crystals. The induction of gout was confirmed by conducting uric acid test as well as by measuring the diameter of the ankle joint. The results of total protein estimation depicted the significant (*P* < 0.001) increase in values. This might be due to an increased level of inflammation in the synovial joint because of MSU crystal accumulation [40].

**Table 4** Results of ROS and TBARS activity of CuONP-administered BALB/c mice

Groups ( <i>n</i> = 6)	Parameter	
	ROS (U/g tissue)	TBARS (nmol/min/mg)
Control	3.31 ± 0.3	3.59 ± 0.3
MSU group	6.80 ± 0.4 ***	16.54 ± 0.4***
CuO-NP-I	2.27 ± 0.1**	2.26 ± 0.2*
CuO-NP-II	1.95 ± 0.2*	2.92 ± 0.2
CuO-NP-III	1.66 ± 0.3***	1.97 ± 0.3***
Allopurinol	2.92 ± 0.5	3.19 ± 0.2

Values are expressed as mean ± SD

\**P* < 0.05

\*\**P* < 0.01

\*\*\**P* < 0.001

**Table 5** Results of total protein estimation of CuONP-administered BALB/c mice

Group ( <i>n</i> = 6)	Parameter
	Protein estimation (mg/g of tissue)
Control	23.81 ± 0.4
MSU group	50.24 ± 1.0 ***
CuO-NP-I	22.57 ± 0.5
CuO-NP-II	24.38 ± 0.3
CuO-NP-III	24.70 ± 0.2
Allopurinol	24.72 ± 0.3

Values are expressed as mean ± SD

\**P* < 0.05

\*\**P* < 0.01

\*\*\**P* < 0.001

The biological system of the cell gets disturbed due to excessive oxidative stress. Previous studies revealed that administration of CuO-NPs will reduce the oxidative stress due to its antioxidant property [41]. In this study, gout was induced by using xanthine oxidase inhibitor known as monosodium urate crystals. The symptoms that appeared later were significantly increased (*P* < 0.001) in ROS and TBARS indicating an induction of gout and increased oxidative stress due to overproduction of oxygen radicals [42]. The allopurinol-treated positive control group showed no significant changes in SOD and POD values as it has the ability to reduce oxidative stress by inhibiting xanthine oxidase (XO) enzyme [43]. The high doses of CuO-NPs increase the SOD, POD, and CAT values while causing a decrease in ROS and TBARS values. Antioxidant activity gets increased due to the high levels of SOD, POD, and CAT. Low levels of ROS and TBARS in the CuO-NP-III group showed that they are important for scavenging the free radicals and boosting the antioxidant activity [41]. It has been reported that copper inhibits XOD activity and suppresses the formation of uric acid effectively. Similarly, a previous study also observed a significant decrease in serum uric acid levels upon the oral administration of turmeric and zinc oxide nanoparticles [44, 45]. It has been concluded from the present experiment that when hyperuricemic or gouty arthritic mice are orally administered CuO-NPs, it will significantly improve the levels of protein and decrease oxidative stress. From this study, it can be concluded that in the coming future, commercially available drug such as allopurinol can be replaced by CuO-NP-containing drug as the prolonged use of allopurinol has major side effects. Furthermore, CuO-NP efficacy has no changes in histopathology of the liver, muscles, and kidney.

**Acknowledgements** The authors are grateful to the International Islamic University, Islamabad, Pakistan, Quaid-e-Azam University, Islamabad, Pakistan, Riphah International University, Islamabad, and National Institute of Health, Islamabad Pakistan for providing the animal house facility.

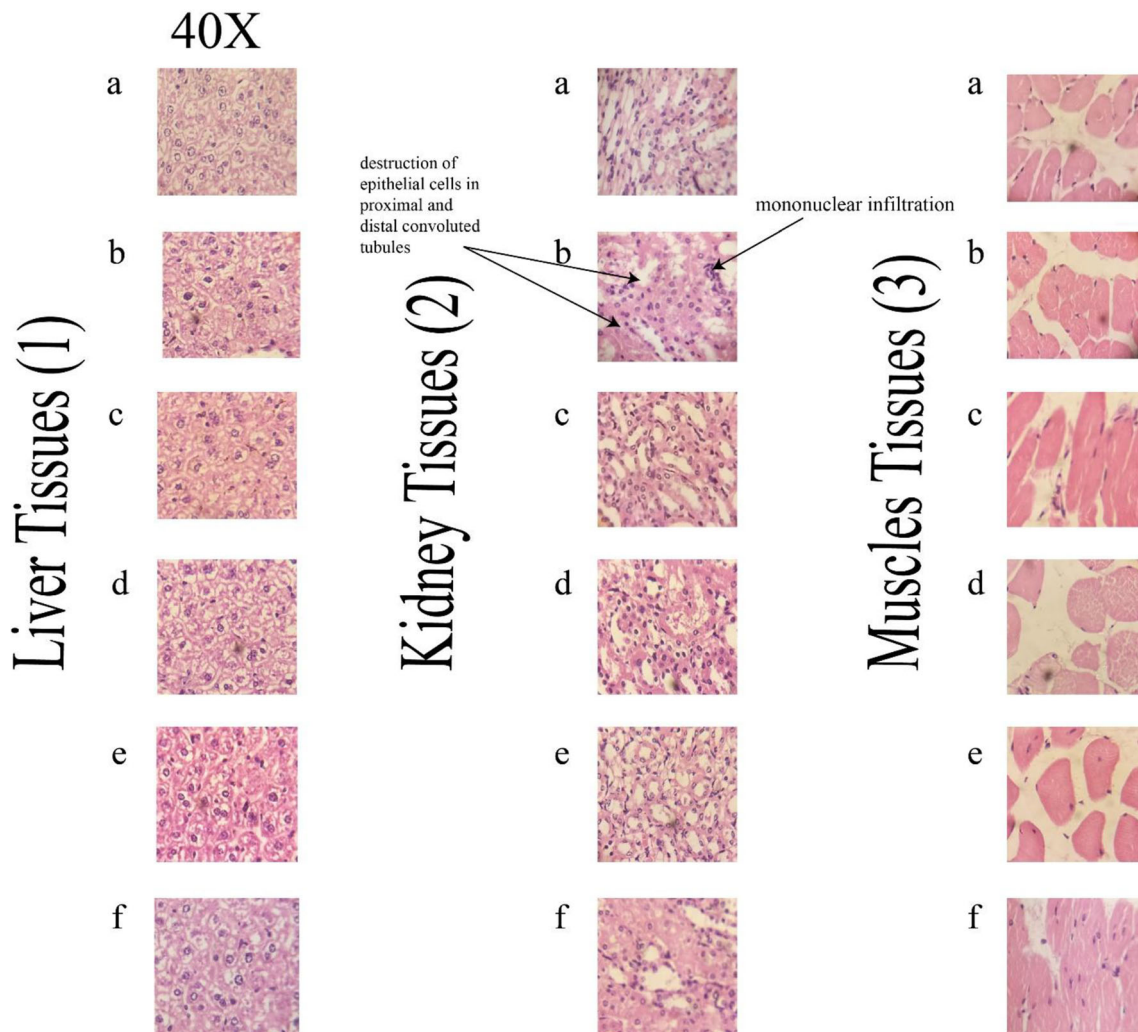


**Fig. 5** Histopathological slides (40X) of mouse liver, kidney, and muscle tissues in which “a” is the normal control, “b” is the MSU group, “c” is the CuONP-I, “d” is the CuONP-II, “e” is the CuONP-III, and “f” is the allopurinol control

## Declarations

**Conflict of Interest** The authors declare no competing interests.

## References

- Tran QH, Le AT (2013) Silver nanoparticles: synthesis, properties, toxicology, applications and perspectives. *Adv Nat Sci Nanosci Nanotechnol* 4(3):033001. <https://doi.org/10.1088/2043-6254/aad12b>
- Iravani S, Korbekandi H, Mirmohammadi SV, Zolfaghari B (2014) Synthesis of silver nanoparticles: chemical, physical and biological methods. *Res Pharm Sci* 9(6):385
- Zhang Z, Kleinstreuer C, Donohue JF, Kim CS (2005) Comparison of micro- and nano-size particle depositions in a human upper airway model. *J Aerosol Sci* 36(2):211–233. <https://doi.org/10.1016/j.jaerosci.2004.08.006>
- Agnihotri S, Mukherji S, Mukherji S (2014) Size-controlled silver nanoparticles synthesized over the range 5–100 nm using the same protocol and their antibacterial efficacy. *RSC Adv* 4(8):3974–3983. <https://doi.org/10.1039/C3RA44507K>
- Duffin R, Tran L, Brown D, Stone V, Donaldson K (2007) Proinflammatory effects of low-toxicity and metal nanoparticles in vivo and in vitro: highlighting the role of particle surface area and surface reactivity. *Inhal Toxicol* 19(10):849–856. <https://doi.org/10.1080/08958370701479323>
- Katz E, Willner I (2004) Integrated nanoparticle–biomolecule hybrid systems: synthesis, properties, and applications. *Angew Chem Int Ed* 43(45):6042–6108. <https://doi.org/10.1002/anie.200400651>
- Soren S, Kumar S, Mishra S, Jena PK, Verma SK, Parhi P (2018) Evaluation of antibacterial and antioxidant potential of the zinc oxide nanoparticles synthesized by aqueous and polyol method. *Microb Pathog* 119:145–151. <https://doi.org/10.1016/j.micpath.2018.03.048>
- Lu PJ, Huang SC, Chen YP, Chiueh LC, Shih DYC (2015) Analysis of titanium dioxide and zinc oxide nanoparticles in cosmetics. *J Food Drug Anal* 23(3):587–594. <https://doi.org/10.1016/j.jfda.2015.02.009>
- Salem SS, Fouda A (2020) Green synthesis of metallic nanoparticles and their prospective biotechnological applications: an overview. *Biol Trace Elem Res*. <https://doi.org/10.1007/s12011-020-02138-3>

10. Busso N, So A (2010) Gout. Mechanisms of inflammation in gout. *Arthritis Res Ther* 12(2):206. <https://doi.org/10.1186/ar2952>
11. Zhang QB, Qing YF, Yin CC, Zhou L, Liu XS, Mi QS, Zhou JG (2018) Mice with miR-146a deficiency develop severe gouty arthritis via dysregulation of TRAF 6, IRAK 1 and NALP3 inflammasome. *Arthritis Res Ther* 20(1):1–9. <https://doi.org/10.1186/s13075-018-1546-7>
12. Peng YJ, Lee CH, Wang CC, Salter DM, Lee HS (2012) Pycnogenol attenuates the inflammatory and nitrosative stress on joint inflammation induced by urate crystals. *Free Radic Biol Med* 52(4):765–774. <https://doi.org/10.1016/j.freeradbiomed.2011.12.003>
13. Cillero-Pastor B, Martín MA, Arenas J, López-Armada MJ, Blanco FJ (2011) Effect of nitric oxide on mitochondrial activity of human synovial cells. *BMC Musculoskelet Disord* 12(1):42. <https://doi.org/10.1186/1471-2474-12-42>
14. Afonso V, Champy R, Mitrovic D, Collin P, Lomri A (2007) Reactive oxygen species and superoxide dismutases: role in joint diseases. *Joint Bone Spine* 74(4):324–329. <https://doi.org/10.1016/j.jbspin.2007.02.002>
15. Zhang DX, Gutterman DD (2007) Mitochondrial reactive oxygen species-mediated signaling in endothelial cells. *Am J Phys Heart Circ Phys* 292(5):H2023–H2031. <https://doi.org/10.1152/ajpheart.01283.2006>
16. Cordero MD (2011) Oxidative stress in fibromyalgia: pathophysiology and clinical implications. *Reumatol Clin* 7(5):281–283. <https://doi.org/10.1016/j.reuma.2010.12.007>
17. Ning JL, Mo LW, Lai XN (2010) Low-and high-dose hydrogen peroxide regulation of transcription factor NF-E2-related factor 2. *Chin Med J* 123(8):1063–1069. <https://doi.org/10.3760/cma.j.issn.0366-6999.2010.08.016>
18. Chenevier-Gobeaux C, Lemarechal H, Bonnefont-Rousselot D, Poiraudau S, Ekindjian OG, Borderie D (2006) Superoxide production and NADPH oxidase expression in human rheumatoid synovial cells: regulation by interleukin-1 $\beta$  and tumour necrosis factor- $\alpha$ . *Inflamm Res* 55(11):483–490. <https://doi.org/10.1007/s00011-006-6036-8>
19. Kurz B, Steinhagen J, Schünke M (1999) Articular chondrocytes and synoviocytes in a co-culture system: influence on reactive oxygen species-induced cytotoxicity and lipid peroxidation. *Cell Tissue Res* 296(3):555–563. <https://doi.org/10.1007/s004410051317>
20. Lin S, Zeng L, Zhang G, Liao Y, Gong D (2017) Synthesis, characterization and xanthine oxidase inhibition of Cu (II)–chrysin complex. *Spectrochim Acta A Mol Biomol Spectrosc* 178:71–78. <https://doi.org/10.1016/j.saa.2017.01.056>
21. Konstantinova SG, Russanova IE, Russanov EM (1991) Do the copper complexes of histamine, histidine and of two H<sub>2</sub>-antagonists react with O<sup>2-</sup>? *Free Radic Res Commun* 12(1):215–220. <https://doi.org/10.3109/10715769109145789>
22. Acharyulu NPS, Dubey RS, Swaminadham V, Kollu P, Kalyani RL, Pammi SVN (2014) Green synthesis of CuO nanoparticles using *Phyllanthus amarus* leaf extract and their antibacterial activity against multidrug resistance bacteria. *Int J Eng Res Technol* 3(4). <https://www.ijert.org/green-synthesis-of-cuo-nanoparticles-using-phyllanthus-amarus-leaf-extract-and-their-antibacterial-activity-against-multidrug-resistance-bacteria>. Accessed 21 Aug 2020
23. Burk RF, Levander OA, Shils ME, Shike M, Ross AC, Caballero B, Cousins RJ (2006) Modern nutrition in health and disease, 312–325. <https://www.ars.usda.gov/research/publications/publication/?seqNo115=154947>. Accessed 23 Aug 2020
24. Lebow ST, Foster D (2005) (2005). Environmental concentrations of copper, chromium, and arsenic released from a chromated-copper-arsenate-(CCA-C-) treated wetland boardwalk. *For Prod J* 55(2):62–70
25. Nguyen XT, Tran TH, Cojoc D, Legname G (2019) Copper binding regulates cellular prion protein function. *Mol Neurobiol* 56(9): 6121–6133. <https://doi.org/10.1007/s12035-019-1510-9>
26. Li LZ, Zhou GX, Li J, Jiang W, Liu BL, Zhou W (2018) Compounds containing trace element copper or zinc exhibit as potent hyperuricemia inhibitors via xanthine oxidase inactivation. *J Trace Elem Med Biol* 49: 72–78. <https://doi.org/10.1016/j.jtemb.2018.04.019>
27. Kiyani MM, Rehman H, Hussain MA, Jahan S, Afzal M, Nawaz I et al (2020) Inhibition of hyperuricemia and gouty arthritis in BALB/c mice using copper oxide nanoparticles. *Biol Trace Elem Res* 193(2):494–501. <https://doi.org/10.1007/s12011-019-01734-2>
28. Hassan SED, Salem SS, Fouda A, Awad MA, El-Gamal MS, Abdo AM (2018) New approach for antimicrobial activity and bio-control of various pathogens by biosynthesized copper nanoparticles using endophytic actinomycetes. *J Radiat Res Appl Sci* 11(3):262–270. <https://doi.org/10.1016/j.jrras.2018.05.003>
29. Khan A, Rashid A, Younas R, Chong R (2016) A chemical reduction approach to the synthesis of copper nanoparticles. *Int Nano Lett* 6(1):21–26. <https://doi.org/10.1007/s40089-015-0163-6>
30. Reeves PG, Nielsen FH, Fahey GC Jr (1993) AIN-93 purified diets for laboratory rodents: final report of the American Institute of Nutrition ad hoc writing committee on the reformulation of the AIN-76A rodent diet. <https://doi.org/10.1093/jn/123.11.1939>
31. Nishimura A, Akahoshi T, Takahashi M, Takagishi K, Itoman M, Kondo H et al (1997) Attenuation of monosodium urate crystal-induced arthritis in rabbits by a neutralizing antibody against interleukin-8. *J Leukoc Biol* 62(4):444–449. <https://doi.org/10.1002/jlb.62.4.444>
32. Chance B, Maehly AC (1955) [136] Assay of catalases and peroxidases. <https://www.sciencedirect.com/science/article/pii/S0076687955023008>. Accessed 9 Sept 2020
33. Kakkar P, Das B, Viswanathan PN (1984) A modified spectrophotometric assay of superoxide dismutase. <http://nopr.niscair.res.in/handle/123456789/19932>. Accessed 9 Sept 2020
34. Wright D, Sutherland L (2008) Antioxidant supplementation in the treatment of skeletal muscle insulin resistance: potential mechanisms and clinical relevance. *Appl Physiol Nutr Metab* 33(1):21–31
35. Hayashi I, Morishita Y, Imai K, Nakamura M, Nakachi K, Hayashi T (2007) High-throughput spectrophotometric assay of reactive oxygen species in serum. *Mutat Res Genet Toxicol Environ Mutagen* 631(1):55–61. <https://doi.org/10.1016/j.mrgentox.2007.04.006>
36. Yang JG, Zhou YL, Okamoto T, Bessho T, Satake S, Ichino R, Okido M (2006) Preparation of oleic acid-capped copper nanoparticles. *Chem Lett* 35(10):1190–1191. <https://doi.org/10.1246/cl.2006.1190>
37. Yang JG, Okamoto T, Ichino R, Bessho T, Satake S, Okido M (2006) A simple way for preparing antioxidation nano-copper powders. *Chem Lett* 35(6):648–649. <https://doi.org/10.1246/cl.2006.648>
38. Zhu H, Zhang C, Yin Y (2005) Novel synthesis of copper nanoparticles: influence of the synthesis conditions on the particle size. *Nanotechnology* 16(12):3079
39. Ren G, Hu D, Cheng EW, Vargas-Reus MA, Reip P, Allaker RP (2009) Characterisation of copper oxide nanoparticles for antimicrobial applications. *Int J Antimicrob Agents* 33(6):587–590. <https://doi.org/10.1016/j.ijantimicag.2008.12.004>
40. Martinon F, Pétrilli V, Mayor A, Tardivel A, Tschopp J (2006) Gout-associated uric acid crystals activate the NALP3 inflammasome. *Nature* 440(7081):237–241. <https://doi.org/10.1038/nature04516>
41. Das D, Nath BC, Phukon P, Dolui SK (2013) Synthesis and evaluation of antioxidant and antibacterial behavior of CuO nanoparti-

- cles. *Colloids Surf B: Biointerfaces* 101:430–433. <https://doi.org/10.1016/j.colsurfb.2012.07.002>
42. Watanabe S, Kiyama F, Sakamaki A, Yoshida T, Fukui T (2006) Cerebral oxidative stress and mitochondrial dysfunction in oxonate-induced hyperuricemic mice. *J Health Sci* 52(6):730–737. <https://doi.org/10.1248/jhs.52.730>
43. Mills PC, Smith NC, Harris RC, Harris P (1997) Effect of allopurinol on the formation of reactive oxygen species during intense exercise in the horse. *Res Vet Sci* 62(1):11–16. [https://doi.org/10.1016/S0034-5288\(97\)90172-7](https://doi.org/10.1016/S0034-5288(97)90172-7)
44. Mustafa Kiyani M, Sohail MF, Shahnaz G, Rehman H, Akhtar MF, Nawaz I et al (2019) Evaluation of turmeric nanoparticles as anti-gout agent: modernization of a traditional drug. *Medicina* 55(1):10. <https://doi.org/10.3390/medicina55010010>
45. Kiyani MM, Butt MA, Rehman H, Ali H, Hussain SA, Obaid S et al (2019) Antioxidant and anti-gout effects of orally administered zinc oxide nanoparticles in gouty mice. *J Trace Elem Med Biol* 56:169–177. <https://doi.org/10.1016/j.jtemb.2019.08.012>

**Publisher's Note** Springer Nature remains neutral with regard to jurisdictional claims in published maps and institutional affiliations.